SECTION II. TASK 2. SUBMODEL DEVELOPMENT AND EVALUATION

Objectives

The objectives of this task are to develop or adapt advanced physics and chemistry submodels for the reactions of coal in an entrained-bed and a fixed-bed reactor and to validate the submodels by comparison with laboratory scale experiments.

Task Outline

The development of advanced submodels for the entrained-bed and fixed-bed reactor models will be organized into the following categories: a) Coal Chemistry (including coal pyrolysis chemistry, char formation, particle mass transfer, particle thermal properties, and particle physical behavior); b) Char Reaction Chemistry at high pressure; c) Secondary Reactions of Pyrolysis Products (including gas-phase cracking, soot formation, ignition, char burnout, sulfur capture, and tar/gas reactions); d) Ash Physics and Chemistry (including mineral characterization, evolution of volatile, molten and dry particle components, and ash fusion behavior); e) Large Coal Particle Effects (including temperature, composition, and pressure gradients and secondary reactions within the particle, and the physical effects of melting, agglomeration, bubble formation and bubble transport; f) Large Char Particle Effects (including oxidation); g) SO_x-NO_x Submodel Development (including the evolution and oxidation of sulfur and nitrogen species); and h) SO_x and NO_x Model Evaluation.

II.A. SUBTASK 2.a. - COAL TO CHAR CHEMISTRY SUBMODEL DEVELOPMENT AND EVALUATION

Senior Investigators - David G. Hamblen and Michael A. Serio
Advanced Fuel Research, Inc.
87 Church Street, East Hartford, CT 06108
(203) 528-9806

Objective

The objective of this subtask is to develop and evaluate, by comparison with laboratory experiments, an integrated and compatible submodel to describe the organic chemistry and physical changes occurring during the transformation from coal to char in coal conversion processes.

Accomplishments

A significant amount of work was done in the area of tar transport during the past quarter. The current vapor pressure law does a good job of predicting the relative amounts of the oligomers in each size classification from FIMS pyrolysis experiments. It also does a good job in predicting the direct vaporization of tar in the FIMS apparatus. However, it predicts a shift in the temperature range of the oligomers as the size range increases in the case of bituminous coal pyrolysis/FIMS, which is not observed in the actual data. We believe this results from restricted diffusion of the large oligomers as the coal begins to resolidify. We have developed a few simple approaches to addressing this problem but these have not been fruitful, so far, i.e., we were not able to fix this problem easily without creating problems in the other predictions.

Work was resumed on the addition of polymethylenes to the FG-DVC model. Some predictions were made of the tar hydrogen composition for coals of different rank and compared to measurements made by Freihaut et al. (1988). Good agreement was obtained except for the two lowest rank coals (Zap lignite, Wyodak subbituminous), where the predicted hydrogen composition was too high.

Work also continued on the swelling model. Additional bubble types (sizes) were introduced into the model in order to improve the prediction of surface area. However, this did not lead to better predictions, so other modifications

to the model will be tried.

Work continued on examining a percolation theory approach to doing the network decomposition calculations. A version of the model was developed which incorporates two different types of bonds, the so-called two-σ model. Three important new features in our two-σ percolation theory are: (i) tar vaporization, (ii) molecular weight distribution of monomers, and iii) an approximation which allows the removal of tar. These features are basically treated the same way as in the original DVC model. The Monte Carlo and two-σ predictions of the tar yield and of the coal fluidity data agree reasonably well with each other and with the data.

Work also continued on the rank dependence of the pyrolysis kinetic rates. During the past quarter, the transfer of TG-FTIR data to the Sun microsystems computer was successfully completed. This will allow a faster and more accurate comparison to the data. Criteria were established to assess the degree of fit to the evolution profiles and the yield data. So far, comparisons have been made with Pittsburgh Seam bituminous coal TG-FTIR data from experiments at four different heating rates. In this case, rank dependent kinetics have been determined which provide an excellent fit to the evolution profiles and yields for each heating rate. We will now do a systematic comparison of the same type of data for the remaining Argonne coals.

A comparison was made of intrinsic reactivity measurements for Montana Rosebud coal determined from the non-isothermal test to the plot developed by Smith (1982) for a range of carbons over a wide range of temperatures. The agreement at low temperatures was within a factor of two when compared to Smith's data for brown coal chars. When the results were extrapolated to high temperatures using E = 35 kcal/mole, again good agreement was obtained with Smith's data for coal chars (within a factor of two).

Tar Transport Model

The tar transport model assumes that the tars reach their equilibrium vapor pressure in the light gases and evolve with these gases as they are transported through the pores or by bubble transport. The details of the model are presented in Solomon et al. (1988a). We have used the vapor pressure correlation of

Suuberg et al. (1985) for the equilibrium vapor pressure. Since this vapor pressure law is a function of molecular weight and temperature, we tested the accuracy of our model in predicting the evolution of tar fragments of specific molecular weight as a function of temperature.

The experimental data used was obtained from FIMS analysis, where the FIMS apparatus is in line with a probe used to heat the sample. The FIMS analysis was performed by Ripudaman Malhotra at SRI International on coals, which pyrolyze in the apparatus (coal FIMS), and on already formed coal tar, which vaporizes in the apparatus (tar FIMS). We divided the tar oligomers (from both data and theory) into five different bins: 50-200 amu, 201-400 amu, 401-600 amu, 601-800 amu, and > 800 amu. The evolution with temperature of each bin is then plotted.

Tar FIMS - We found good agreement between the tar FIMS data and our simulation (Fig. II.A-1). A small mismatch is present for large molecular weight oligomers (> 800 amu), where the maximum of rate evolution occurs later in the simulation. The peak is also narrower, i.e. the temperature range of evolution is shorter than found experimentally. The vaporization of smaller oligomers is, however, well predicted. This validates the temperature and molecular weight dependence of the vaporization law (Suuberg et al., 1985) used in the model but not the absolute magnitude of the vapor pressure.

Coal FIMS - We compared the results of the simulation with coal FIMS data for two coals, Pittsburgh No. 8 and Wyodak. We found the best agreement when the Suuberg et al. (1985) correlation is multiplied by ten. For the Pittsburgh No. 8, the theory gave an accurate prediction for the evolution temperature of low molecular weight oligomers, as well as the relative amounts of all oligomer classes (Fig. II.A-2). It, however, predicted higher evolution temperatures for high molecular weight oligomers (> 600 amu), while the data showed a unique temperature of maximum evolution rates (T_{max}) for all molecular weights. A shift to higher T_{max} with higher molecular weight is consistent with the fact that large oligomers need higher temperatures to vaporize, as confirmed by the tar FIMS data. Since coal FIMS data doesn't present this feature, we suspect some additional limitations occur as the fluid coal melt resolidifies.

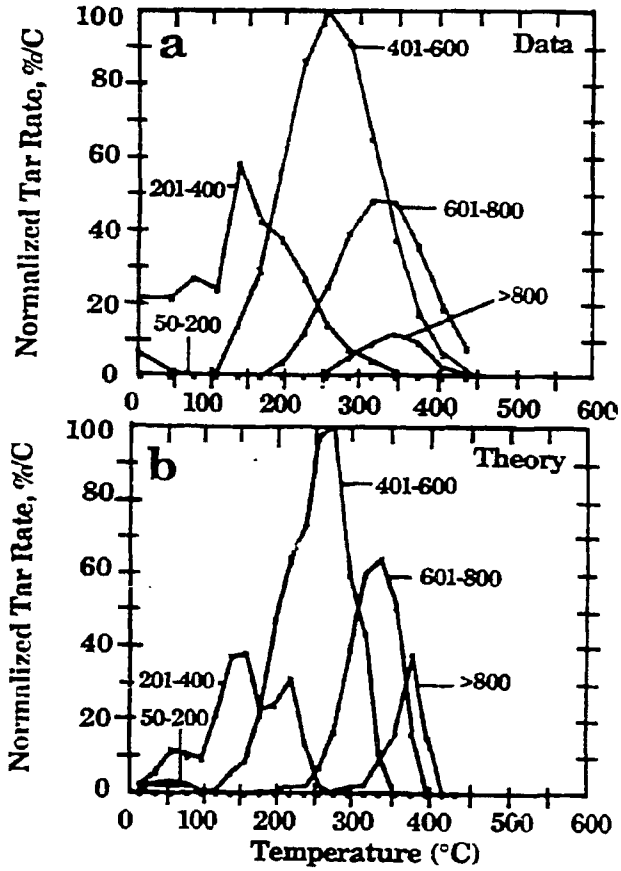

Figure II.A-1. Comparison of a) FIMS Data and b) Theory for Pittsburgh No. 8 Coal Tar.

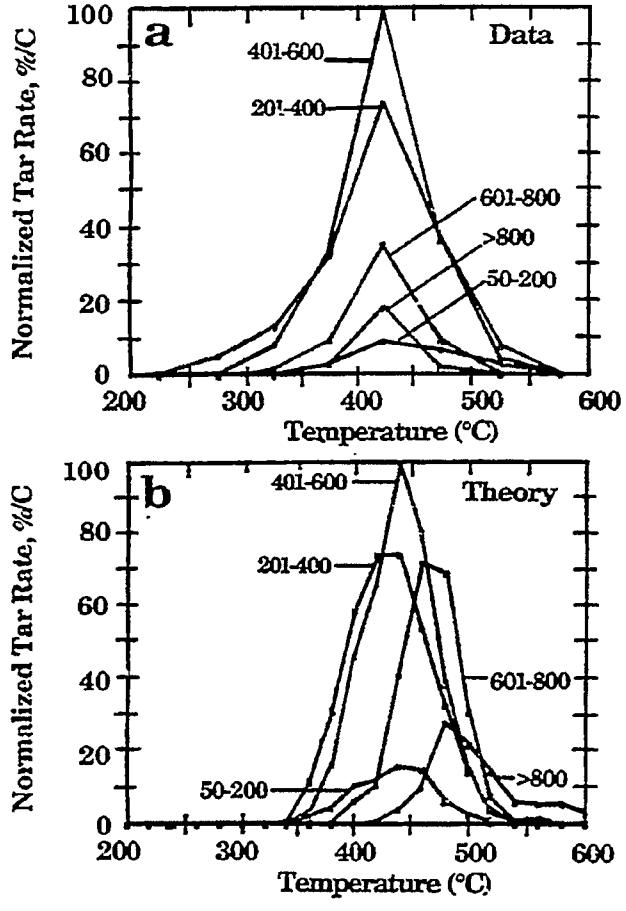

Figure II.A-2. Comparison of a) FIMS Data and b) Theory for Normalized Tar Rate for Pittsburgh No. 8 Coal Pyrolyzed in the FIMS.

The simulation for Wyodak coal gave a good prediction for the evolution of all molecular weight classes oligomers, including large ones (Fig. II.A-3). The data (Fig. II.A-3b) shows that the evolution of high molecular weight oligomers occurs slightly before the smaller oligomers. This also suggests the presence of additional limitations. In our simulation for low rank coals, the peak position is regulated by the low temperature cross-linking rate (which reduces the number of large oligomers which can vaporize) rather than by the vaporization law.

In order to obtain a better prediction for Pittsburgh No. 8, we considered additional transport limitations related to the reduction in the fluidity of the coal. However, none of the simple modifications tried gave a significant improvement in the model for both low and high rank coals. The current model gives good predictions for the relative amounts of the oligomers in each size classification. It also predicts accurately the evolution temperature of low molecular weight (< 600 amu) oligomers. The vapor pressure dependence on temperature and molecular weight is also validated by the good prediction of the tar FIMS data. The present model, therefore, uses the original FG-DVC transport assumption (Solomon et al., 1988a) with the Suuberg et al. (1985) vapor pressure correlation multiplied by ten.

Polymethylenes

Varying amounts (typically 0-9%, but in some cases as high as 18%) of long-chain aliphatics (polymethylenes) have been reported in pyrolysis products by Nelson (1987) and by Calkins and coworkers (1984a,b,c,d) and references quoted therein. The chains appear alone and attached to aromatic nuclei. The presence of these polymethylenes makes the tar more aliphatic than the parent coal. Also, for most coals, there is a low temperature tar peak which results from the vaporization of unattached small polymethylenes plus small aromatic ring clusters. This vaporization peak is illustrated in Fig. II.A-4 (from the Third Annual Report). Polymethylene chains can also crack or be released into the second tar peak. Further cracking of this material under more severe devolatilization conditions produces ethylene, propylene, and butadiene from which the concentration of polymethylenes may be determined (Calkins et al., 1984d). Originally, the polymethylenes were included in the FG model as part of the aliphatic functional group pool, which is assumed to decompose to produce

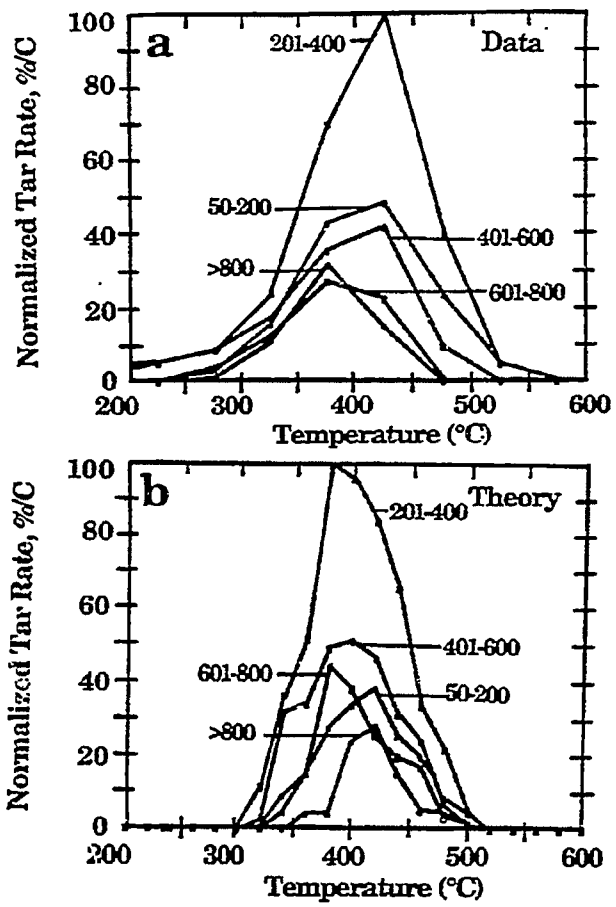

Figure II.A-3. Comparison of a) FIMS Data and b) Theory for Normalized Tar Rate for Wyodak Coal Pyrolyzed in the FIMS.

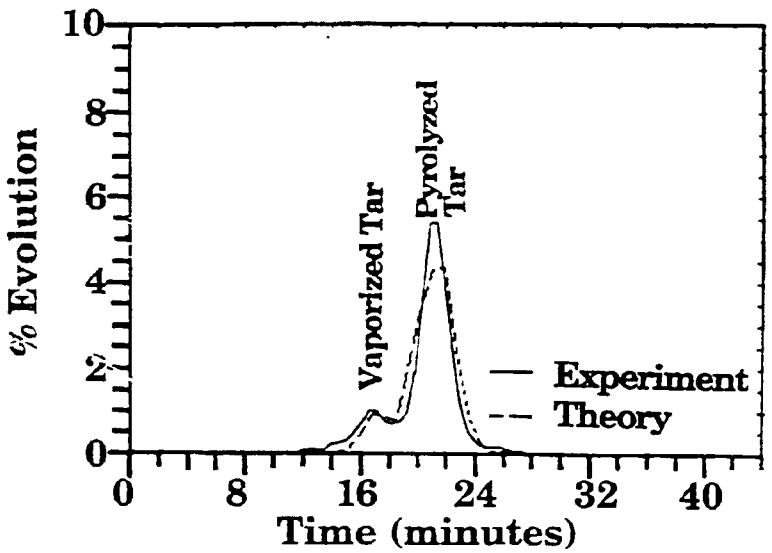

Figure II.A-4. Comparison of FG-DVC Model Predictions for Tar Evolution Rate from Upper Freeport Coal with TG-FTIR Data.

gas products, not tar. This leads to predicted H/C ratios in the tar for low rank coals which are lower than those measured by Freihaut et al. (1988).

Polymethylenes have now been added to the DVC part of the model as a second class of material whose molecular weight distribution and functional group composition are different from the main macromolecular network. The starting coal molecule now includes a distribution of oligomer sizes for polymethylenes and other guest molecules (with the chemical composition of the network). The vaporization of these molecules produces a peak which matches the early vaporization peak as shown in Fig. II.A-4. We also account for polymethylenes which are attached to the coal matrix and removed by bond breaking by including them as species in the FG model. Those polymethylenes are then added to the tar after vaporization.

The model requires a value for the total polymethylene content in the coal. Calkins determined that the yields of ethylene, butadiene, and propylene correlated well with the polymethylene content (1984d). It was decided that this is the most general and fruitful approach to take and we have used the coals which are in our set and Calkins' set to calibrate the method. As a first approximation, we arbitrarily chose to use polymethylene = 0.7 (C_2H_4). This gave $-CH_2-$ contents slightly above Calkin's values, but within 15% of Calkin's. The model also assumes that 50% of the polymethylenes are small enough to vaporize and are included in the oligomer pool while the other 50% are not and are included in the FG pool.

A prediction for the total tar yield including polymethylenes is compared in Fig. II.A-4 with measurements from a TG-FTIR experiment (Solomon et al., 1989a). The agreement is good. Comparisons between the predicted and measured (Freihaut et al., 1988) tar hydrogen compositions are shown in Fig. II.A-5. The prediction is good for high rank coals and shows the correct trend with rank. The tar hydrogen composition is, however, overpredicted for lower rank coals. This is due to the fact that the model underpredicts, for these coals, the tar yield at high heating rates. The relative contribution of polymethylenes is then more important. By improving the tar predictions with adjustments of DVC parameters, we should be able to obtain more accurate values of the tar hydrogen composition.

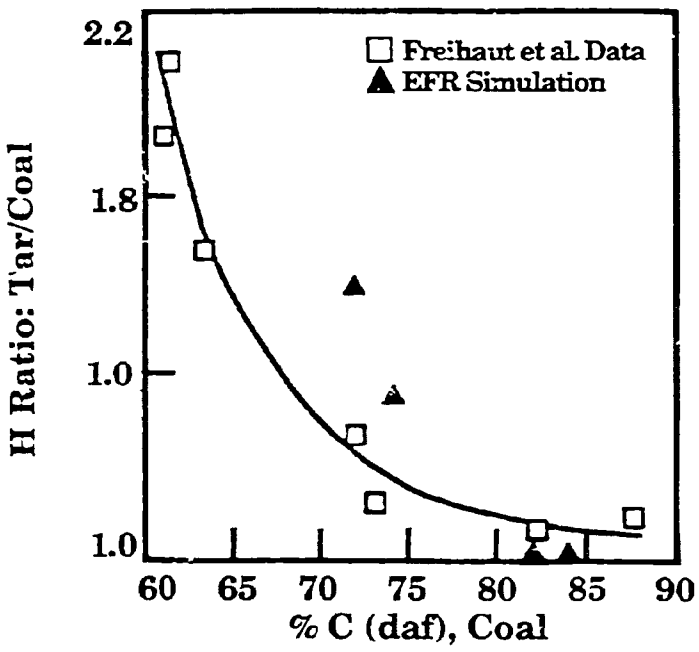

Figure ILA-5. Ratio of % H in Tar to % H in Coal as a Function of Coal Rank. (from Freihaut et al. (1988).

Swelling Model

Work also continued on the swelling model. We recently developed a multibubble approach to doing the swelling predictions. Since the swelling predictions depend on the fluidity model, some problems were introduced by the statistical variations in the fluidity model. This was solved by using a lookup table for the viscosity values based on averaging the results of several runs. Using a multi-bubble model with a single bubble size, reasonable predictions have been obtained for data on the swelling ratio and the porosity but not for surface area (too low). Additional bubble types (sizes) were introduced into the model in order to improve the prediction of surface area. However, this did not lead to better predictions, so other modifications to the model will be tried. The predictions are sensitive to the number of starting bubbles.

Percolation Theory

The statistical Monte Carlo method used in our FG-DVC model has been quite successful in predicting the depolymerization and crosslinking processes of the coal macromolecular network. However, the method has a few drawbacks. First, it is computationally time-consuming compared with other statistical methods. Second, its statistical nature presents a certain degree of fluctuation in the final results. The latter becomes increasingly significant and poses some difficulties for the modeling of coal fluidity and swelling.

To address these problems, attempts have been made to use the mathematics of percolation theory as an alternative to Monte Carlo calculations (Solomon et al., 1989b; Niksa and Kerstein, 1987; Grant et al., 1989). Percolation theory gives closed-form solutions for a Bethe lattice. Keeping in mind that an actual coal network contains some different features from the Bethe lattice (e.g. the Bethe lattice has no loops), we made use of some basic concepts of percolation theory while we further modified the mathematics of this theory to describe vaporization processes in coal devolatilization.

One of the key parameters of percolation theory is the coordination number, $\sigma + 1$ which describes the possible number of bridge attachments per ring cluster (monomer). A linear chain has $\sigma + 1 = 2$, while a rectangular "fish net" has $\sigma + 1 = 4$. The higher the coordination number, the more bridges must break to

create network fragments. In attempting to apply percolation theory to the FG-DVC model (Solomon et al., 1989b), it became obvious that the single coordination number lattice used in most applications of percolation theory was not appropriate to describe coal network decomposition. It appears from solvent swelling data (Sanada and Honda, 1966; Larsen and Kovac, 1978; Green et al., 1982; Lucht and Peppas, 1981,1987) and NMR data (Solum et al., 1989), that coal begins as a chain-like material with crosslinks every 2 to 8 ring clusters, i.e., $\sigma + 1$ between 2.2 and 2.5. So, its decomposition requires a low coordination number. However, crosslinking processes can occur at elevated temperature to increase the coordination number. Therefore, we extended the mathematics of percolation theory from a one-dimensional probability computation into a two-dimensional probability computation to describe the coal network as a lattice with two bond types per cluster, i.e., two coordination numbers. This modified theory is referred to as the two-σ model (Solomon et al., 1989b).

Two important new features in our two-σ percolation theory are: (i) tar vaporization and (ii) the molecular weight distribution of monomers. These features are basically treated the same way as in the original DVC model. The molecular weight of monomers is described by a probability distribution, which allows for the fact that monomers are made of various multi-ring structures. Tar molecules are removed out of the coal network using Suuberg's modified vaporization law. Molecular weight distributions of tar and char are kept track of during pyrolysis by a bookkeeping of the vaporization process in each mass bin. The percolation theory gives the mass fraction of all n-mers during pyrolysis. Combining this with a given molecular weight distribution of monomers, one can obtain the mass fraction of coal in each mass bin, which consists of two components: char and tar. Tar vaporization is computed for each mass bin. Tar in each mass bin monotonically increases and reduces the amount of char available for vaporization in the same bin until the char bin is emptied. Figure II.A-6 shows the comparison of predicted tar yields between the Monte Carlo method and the modified percolation theory. Also, a two-σ prediction of the fluidity for the same coal is included in Fig. II.A-7. The Monte Carlo and two-σ predictions agree reasonably well with each other and with the data.

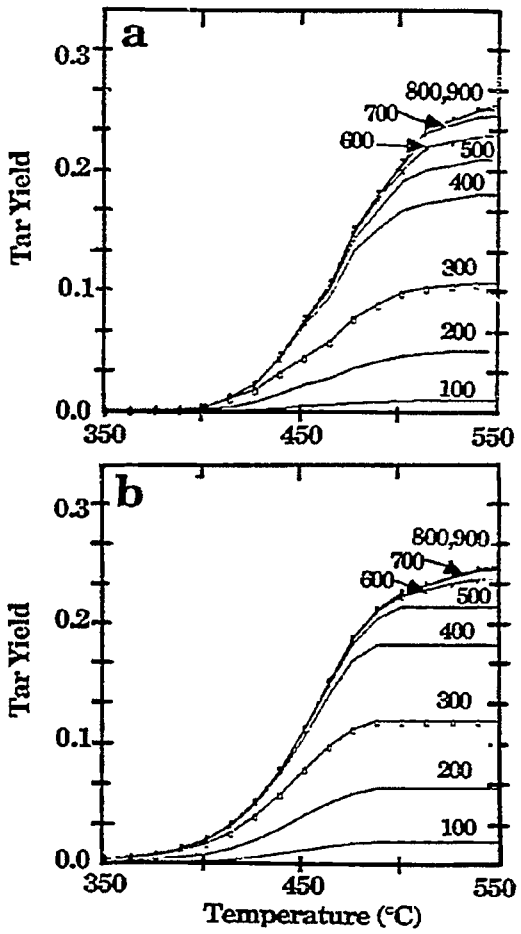

Figure II.A-6. Comparison of Tar Molecular Weight Distributions Predicted with: a) Monte Carlo Method and b) Two-σ Percolation Theory.

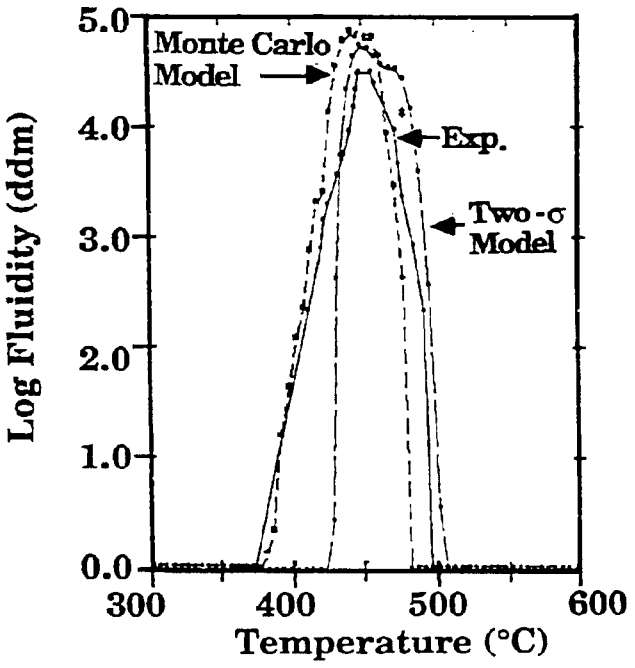

Figure II.A-7. Fluidity of Upper Freeport Coal: Experiment (solid), Monte Carlo Theory (dashed) and Percolation Theory (long dashed).

Rank Dependent Pyrolysis Kinetics

Work also continued on the rank dependence of the pyrolysis kinetic rates. During the past quarter, the transfer of TG-FTIR data to the Sun microsystems computer was successfully completed. This will allow a faster and more accurate comparison to the data. Criteria were established to assess the degree of fit to the evolution profiles and the yield data. So far, comparisons have been made with Pittsburgh Seam bituminous coal TG-FTIR data from experiments at four different heating rates. In this case, rank dependent kinetics have been determined which provide an excellent fit to the evolution profiles and yields for each heating rate. We will now do a systematic comparison of the same type of data for the remaining Argonne coals.

Correlation of T_{cr} Measurements with High Temperature Combustion Reactivities

A non-isothermal reactivity test has been used to make measurements of the critical temperature, T_{cr}, which is an index of relative char reactivities (Solomon et al., 1986; Serio et al., 1990). Of course the measurement of T_{cr} would not be of much good to those interested in p.f. combustion unless it can be shown that these measurements correlate with intrinsic reactivities measured at high temperatures. The T_{cr} measurement provides a temperature at which df/dt = 0.001 s^{-1}. For a - 60 μm mean diameter fraction of Montana Rosebud coal, the measured T_{cr} was 429°C (702K) while the measured CO_2 surface area was 152 m^2/g. The problems of using the BET surface area as a correlating parameter have been discussed previously (Best et al., 1987; Serio et al., 1989). However, since the intrinsic reactivity (R_i) data in the literature have been derived using such measurements, this approach is consistent. The CO_2 area varies the least over a wide range of burnoffs, for most coal chars, and is used here. Using the CO_2 surface area, one would calculate $R_i = 1.1 \times 10^{-10} g/cm^2 s$ at T_p = 702 K. The most comprehensive compilation of intrinsic reactivity data for a range of carbons is that provided by Smith (1982). The correlation of Smith would predict a value of $R_i = 1.0 \times 10^{-11}$ g/cm^2 s. However, this correlation underpredicts the data for brown coal chars and lignites in this temperature range, so the agreement is actually within a factor of 2 of the relevant data in Fig. 9 of Smith (1982). The extrapolation to high temperatures can be done by using E = 35 kcal/mole which gives $R_i = 2 \times 10^{-4}$ $g/cm^2 s$ at T_p = 1650K. This estimate is about a factor of two lower than Smith's correlation and about a factor of two higher than his data

for brown coal chars. A similar agreement is observed for the other chars that were studied. Consequently, it appears that the T_{α} measurement is capable of giving meaningful results when extrapolated to high temperatures using an activation energy of E = 35 kcal/mole.

Recent work in our laboratory with a laminar coal flame experiment has shown a correlation of T_{α} with the ignition point above the nozzle (Solomon et al., 1988b) and with the interval of time required to achieve 100% burnout (Solomon et al., 1989c).

Plans

The work on the development of rank dependent parameters will be continued for the rest of the Argonne coals. In addition, the work on the swelling model and the development of the percolation theory approach will also be continued. Work will be initiated on studying the evolution of sulfur and nitrogen species.

II.B. SUBTASK 2.B. - FUNDAMENTAL HIGH-PRESSURE REACTION RATE DATA

Senior Investigators - Geoffrey J. Germane and Angus U. Blackham
Brigham Young University
Provo, Utah 84602
(801) 378-2355 and 6536

Student Research Assistants - Charles Monson, Russell Daines, and Gary Pehrson

Objectives

The overall objective of this subtask is to measure and correlate reaction rate coefficients for pulverized-coal char particles as a function of char burnout in oxygen at high temperature and pressure.

Accomplishments

Three components of the subtask have been identified to accomplish the objectives outlined above: 1) develop the laminar-flow, high-pressure, controlled-profile (HPCP) reactor, 2) prepare char at high temperature and pressure, and 3) determine the kinetics of char-oxygen reactions at high pressure. The HPCP reactor, capable of functioning at 400 psi (27 atmospheres), has been constructed to perform the fundamental reaction rate measurements required for the study. Data from another char oxidation study (atmospheric pressure) conducted at Brigham Young University will also be used.

Work continued during the last quarter on development of the high-pressure, controlled-profile (HPCP) reactor, the preparation and characterization of char, and the kinetics of char oxidation at high pressure. Most of the effort focused on development of the facility and analytical techniques in preparation for completion of the comprehensive test program. Some coal devolitalization tests of a coal identified for this study were conducted in connection with an independent research program, which has participated financially in the development of advanced instrumentation for the HPCP.

High Pressure Reactor Development and Characterization

Reactor Configuration - Following the initial reactor characterization and char tests, some modifications were found necessary to improve the operation of the reactor and the accuracy of the results. Many of these modifications were initiated during this reporting period, and are described below. Electronic mass flow meters were added to monitor the collection probe quench gas. The flow rate of this particular stream was difficult to obtain accurately when determined by difference using the total exit flow and the other inlet flows. Automatic control valves are being added to the inlet mass flow meters to allow easier stabilization and more consistent flow rates at elevated pressure. A smaller, water-cooled injection probe is also being fabricated. This new probe will have an outer diameter of 9.5 mm compared to an outer diameter of 13 mm for the original probe. The smaller size will allow the injection probe to be better insulated, which will reduce the load on the wall heaters and decrease the temperature drop of the gas flowing through the reaction tube.

In the past, gas temperatures have been measured with an unshielded, platinum-rhodium thermocouple that was inserted through the injection probe and moved along the centerline of the reaction tube. It was found that this probe resulted in temperatures approximately 50 K hotter than a radiation shielded probe inserted from the bottom of the reactor. The difference was due to both radiation and the large temperature gradient in the thermocouple leads as they entered the cooled injection probe. In order to obtain more accurate gas temperature measurements, a water-cooled, radiation-shielded suction pyrometer has been designed, and its fabrication is nearly complete. The test facility has also been modified to enable insertion of the suction pyrometer from the bottom of the reactor to provide gas temperature measurements along the reaction tube centerline without disturbing the upstream flow. Gas temperatures in the collection probe will also be obtained, providing information on quenching effectiveness.

Collection System - Under separate funding, the char/tar/gas separation and collection system is being modified to improve the separation and collection of tar, char and gas. Initial NMR analyses from collected tar samples indicated that the quench occurring in the collection probe has not been consistently sufficient to prevent secondary reactions. Further, a mass balance revealed that approximately 10 percent of the total collected tar was

found on the end of the collection probe that was without transpiration cooling, and on the walls of the impactor.

In order to improve collection efficiency, the collection probe is being redesigned to enhance the initial quench as the combustion particles exit the reaction zone to arrest all secondary reactions, and to lengthen the area of transpiration through the entire length of the collection probe to reduce the agglomeration of tar on the collection probe walls. In addition, the virtual impactor is being redesigned to reduce both the recirculation zones and the internal surface area to diminish the amount of tar sticking to the walls and to reduce the amount of char which collects before the cyclone. A backflush system is also being added to the cyclone to enhance char particle scavenging at low reactor pressure. Figure II.B-1 shows the modified collection system.

Char Preparation at High Temperature and High Pressure

Four devolatization runs were made on a North Dakota lignite to test the tar-char collection procedures. The runs were made at 1250 K and 1235 K, at pressures of 1 and 5 atmospheres, and at residence times of 50 and 200 ms. The distribution of the tar and char fractions are indicated in Table II.B-1. Two values for the tar, from two flow paths, are given in Runs 2-4. Path 1 carries the tar on the outside of the central tube in the impactor and is collected on a downstream filter. Path 2 carries the aerosol that goes through the central tube of the impactor and does not remain in the cyclone with the char, but is collected downstream of the cyclone on a separate filter. The tar and char fractions were analyzed for selected elements to determine whether or not any of these elements were selectively concentrated in either the tar or char fractions. Table II.B-1 shows percentages of calcium and iron in the tar and char fractions along with CHN analyses for these fractions. The detailed interpretations of these data are being made as part of a related, independent project.

From a previous determination of titanium content of a series of replicate samples it was observed that slight shifts in responses from the inductively-coupled plasma instrument for particular elements during analysis of several samples necessitated more frequent calibration. In this way the precision of the measurements has been improved. This will have application as additional oxidation kinetic runs are made in which the extent of reaction is measured by the titanium content of the oxidized chars.

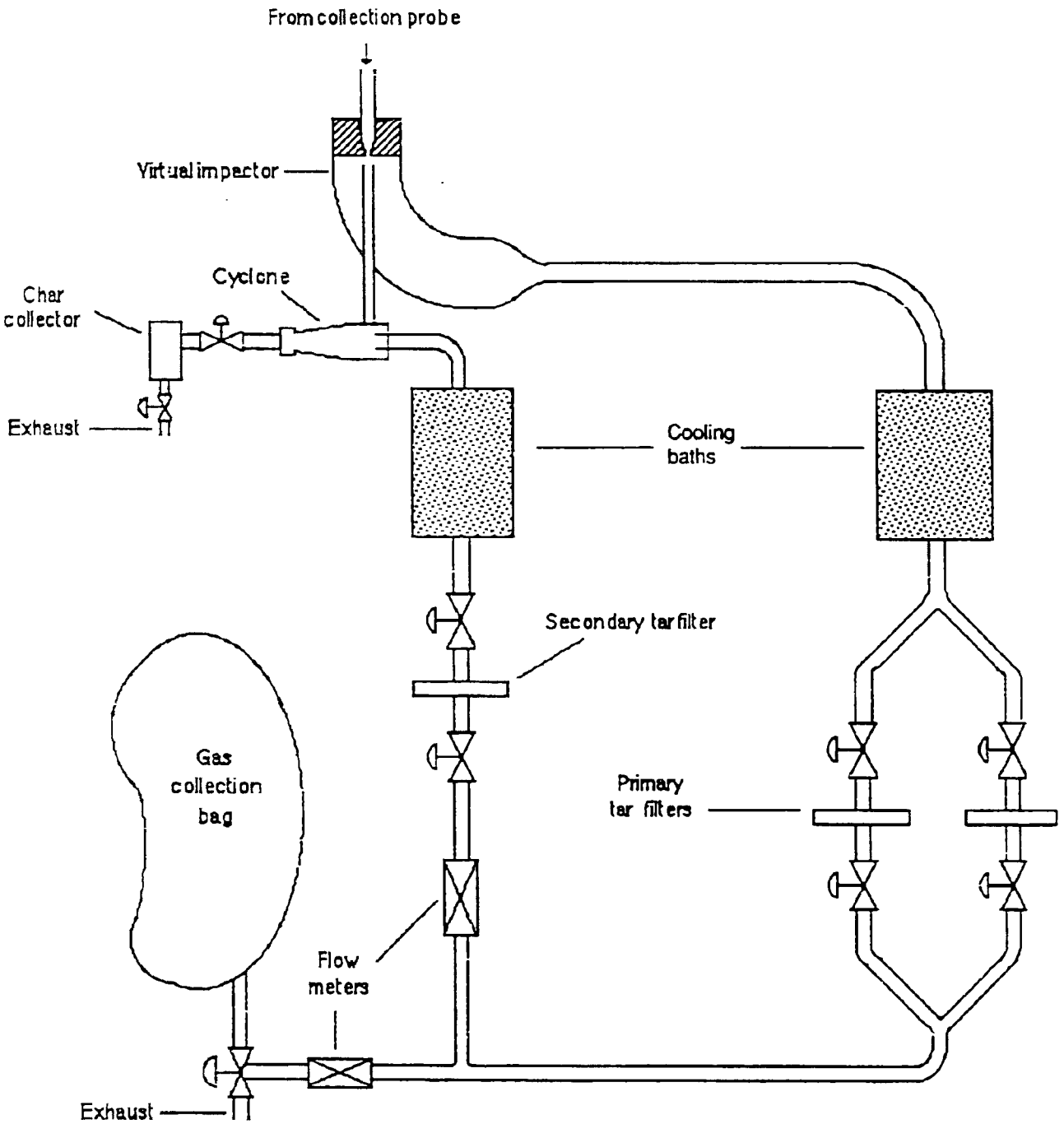

Figure II.B-1. Schematic of char/tar/gas separation and collection system.

Table II.B-1. Devolatilization of a North Dakota Lignite for Tar-Char Production

Run				Mass of Products (mg)	Tar Analyses (%)				
	Reaction Conditions								
No.	Pressure (atm)	Temp (k)	Residence Time (ms)	1. Tar-Path 1 2. Tar-Path 2 3. Char	Calcium	Iron	Carbon	Hydrogen	Nitrogen
1	1	1250	50	161	0.83	1.04			
				---	----	----			
				390	1.48	2.10	62.25	3.84	1.66
2	1	1250	50	180	0.82	1.08			
				40	1.19	1.77			
				974	1.29	2.08	62.19	3.70	1.51
3	5	1235	200	186	1.09	1.63			
				42	1.06	1.93			
				1360	1.26	2.40	61.93	3.58	1.61
4	5	1250	50	194	0.81	1.07			
				21	1.47	2.34			
				467	1.41	2.45	63.83	3.35	1.49
Coal					1.26	1.92	60.38	4.08	1.71

Kinetics of Char-Oxygen Reactions at High Pressure

Mitchell (1989) reported that char particles of the same size undergoing the same conditions have large variations in temperature and burning times. Samples of the same coal with most of the mineral matter removed exhibited a reduction in temperature and burning time variation. Mitchell concluded that variations in the ash content of the char were responsible for the differences in combustion. Catalytic effects of the mineral matter appeared to have little effect since the raw coal and cleaned samples both exhibited the same temperature dependence. Evidence was also found that the traditional kinetic model for char combustion may not be valid. These results may be very useful in helping to interpret results from the present study, since individual particle measurements of temperature will be made during char oxidation and extent of reaction will be determined from the collected particles.

Plans

The modifications to the HPCP reactor discussed previously will be completed during the next quarter. Completion of the suction pyrometer will allow better characterization of gas temperatures in the reaction tube. Previous conditions used for devolatilization and char oxidation experiments will be duplicated and temperature profiles will be measured to better characterize the particle temperatures encountered during the experiments. Components for the pyrometry and particle imaging system have been ordered and the system will be assembled and calibrated during the next reporting period.

During the upcoming quarter the remainder of the collection system will be reviewed. Based on the flow rates that will be employed in upcoming devolatilization and oxidation runs, design parameters of the cyclone will be determined to optimize collection efficiency of the char particles. To reduce the amount of tar that can condense on the tube walls, between the char separation and the collection filters, alternative methods of cooling the tar/gas flow will be examined. The method which employs the shortest possible length of tubing while maintaining the desired tar collection temperature will be selected.

Scanning electron micrographs of the coal samples used in previous tests indicated that the size classification of the particles needs to be improved. A relatively large number of particles that were smaller than the desired size

fraction were included in the samples because of agglomeration with particles of the desired size. Steps have been or will be taken to improve the sieving process, including prevention of agglomeration with an additive, and particle size measurements will be made with a Coulter counter. Selected devolitalization and char oxidation experiments using tight size fractions of Pittsburgh #8 bituminous and North Dakota lignite coal samples will be repeated. Further char oxidation experiments with these two coals will be conducted at a number of temperatures and elevated pressures.

II.C. SUBTASK 2.c. - SECONDARY REACTION OF PYROLYSIS PRODUCTS AND CHAR BURNOUT SUBMODEL DEVELOPMENT AND EVALUATION

Senior Investigator - James R. Markham and Michael A. Serio
Advanced Fuel Research, Inc.
87 Church Street, East Hartford, CT 06108
(203) 528-9806

Objective

The objective of this subtask is to develop and evaluate by comparison with laboratory experiments, an integrated and compatible submodel to describe the secondary reactions of volatile pyrolysis products and char burnout during coal conversion processes. Experiments on tar cracking, soot formation, tar/gas reactions, char burnout, and ignition will continue during Phase II to allow validation of submodels in Phase II.

Accomplishments

Work continued on doing coal flame experiments in the transparent wall reactor (TWR). An attempt was made to use the Pittsburgh Seam bituminous coal. However, some problems were experienced in feeding the coal and with flame stability. Consequently, a switch was made back to Montana Rosebud subbituminous coal.

For a Montana Rosebud flame, tomographic reconstruction techniques were applied to line-of-sight FT-IR Emission/Transmission (E/T) measurements to derive spectra that correspond to small volumes within a coal flame. From these spectra, spatially resolved point values for species temperatures and relative concentrations can be determined. Values for particle temperature, relative particle density, relative soot concentration, the fraction of ignited particles, the relative radiance intensity, the relative CO_2 concentration and the CO_2 temperature have been obtained as functions of distance from the flame axis and height above the coal injector nozzle. Initial measurements (reported last quarter) were made at 6 cm and 12 cm above the coal injector nozzle, with the ignition point occurring at 10 cm. During this quarter, two more slices of data, at 16 cm and 20 cm above the nozzle were collected and tomographically

reconstructed. An in-depth discussion of the four measurement positions can be found in Appendix A, which is a copy of our paper entitled "FT-IR Emission/ Transmission Tomography of a Coal Flame", which has been submitted to the 23rd Symposium (Int) on Combustion, France, (1990). The spectroscopic data are in good agreement with visual observations and thermocouple measurements. The data present a picture of the coal burning in a shrinking annulus which collapses to the center at the tip of the flame. CO_2 temperatures are highest in the rapid burning zone (2300 to 2900 K). The highest particle temperatures in this zone are 1900 to 2000 K, with temperatures up to 2400 K outside the zone.

Measurements are in progress or planned for 9.5, 10.5, 14, 18, and 25 cm above the nozzle for the Rosebud flame. With the local profiles we plan to produce pseudo-color images of the flame's central plane for temperature and relative concentrations fields in the manner we previously employed for tomography measurements in an ethylene diffusion flame (Ref. 3 in Appendix A).

Plans

Continue with tomography measurements at different heights in coal flames and compare tomography results for different coals. Continue characterization of TWR geometry and interact with BYU on PCGC-2 simulations of this system.

II.D. SUBTASK 2.d - ASH PHYSICS AND CHEMISTRY SUBMODEL

Senior Investigators - James Markham and Michael Serio
Advanced Fuel Research, Inc.
87 Church Street, East Hartford, CT 06108
(203) 528-9806

Objective

The objective of this task is to develop and validate, by comparison with laboratory experiments, an integrated and compatible submodel to describe the ash physics and chemistry during coal conversion processes. AFR will provide the submodel to BYU together with assistance for its implementation into the BYU PCGC-2 comprehensive code.

To accomplish the overall objective, the following specific objectives are: 1) to develop an understanding of the mineral matter phase transformations during ashing and slagging in coal conversion; 2) To investigate the catalytic effect of mineral matter on coal conversion processes. Data acquisition will be focused on: 1) design and implementation of an ash sample collection system; 2) developing methods for mineral characterization in ash particles; 3) developing methods for studying the catalytic effects of minerals on coal gasification.

Accomplishments

The work on the study of mineral transformations in the entrained flow reactor (EFR) was temporarily suspended due to manpower and funding constraints.

Temperature Programmed Desorption (TPD) experiments were done in air for chars produced from all of the Argonne coals. The CO_2 desorption and the O_2 adsorption show a consistent trend with the char reactivity as measured by the Critical Temperature (T_{cr}). The more reactive chars adsorb more O_2 and give off CO_2 earlier. These experiments will be repeated with chars produced from demineralized samples of these coals and experiments will also be done in CO_2.

Samples of char were collected from the Montana Rosebud coal flame experiments in order to do reactivity measurements. Since the samples at high

levels of burnout had high ash contents, the non-isothermal reactivity measurement technique (which determines the "critical" temperature) had to be modified to account for this.

Plans

Continue study of mineral effects on the reactivity of low and high rank coals. Continue analysis of material and element balances from ash collections in the entrained flow reactor.

II.E. SUBTASK 2.e. - LARGE PARTICLE SUBMODELS

Senior Investigator - Michael A. Serio
Advanced Fuel Research, Inc.
87 Church Street
East Hartford, CT 06108
(203) 528-9806

Objective

The objectives of this task are to develop or adapt advanced physics and chemistry submodels for the reactions of "large" coal particles (i.e., particles with significant heat and/or mass transport limitations) and to validate the submodels by comparison with laboratory scale experiments. The result will be coal chemistry and physics submodels which can be integrated into the fixed-bed (or moving-bed) gasifier code to be developed by BYU in Subtask 3.b. Consequently, this task will be closely coordinated with Subtask 3.b.

Accomplishments

The work on the AFR fixed-bed reactor (FBR) system was continued. Experiments were done at two bed depths and two flow rates with samples of Illinois No. 6, Pittsburgh No. 8, and Upper Freeport bituminous coals. Over the range of bed depths examined, there did not appear to be a large effect on tar yield and composition. We were restricted from using larger bed depths because problems with tar deposition in the gas cell. However, the ability to bypass some of the tar from the cell has recently been added which will allow larger samples to be used.

It was also found that the temperature of the maximum evolution rate of tar and CH_4 unexpectedly decreased with increasing bed depth. This was due to low levels of oxygen contamination. The contamination problems have recently been solved.

Plans

Complete initial set of experiments on secondary reaction effects in thick beds. Continue development of single particle model with BYU. Begin work on tar repolymerization model.

II.F. SUBTASK 2.F. - LARGE PARTICLE OXIDATION AT HIGH PRESSURES

Senior Investigators: Angus U. Blackham and Geoffrey J. Germane
Brigham Young University
Provo, Utah 84602
(801) 378-2355 and 6536

Student Research Assistants: Gary Pehrson and Michael Sheetz

Objectives

The overall objective for this subtask is to provide data for the reaction rates of large char particles of interest to fixed-bed coal gasification systems operating at pressure.

The specific objectives for this quarter, which was the first quarter of this study, include:

1. Select personnel for work on this study.
2. Review appropriate literature in pertinent areas.
3. Select the experimental approach.
4. Discuss and evaluate equipment design features.

Accomplishments

Two components of this subtask to accomplish the overall objective were suggested in the Phase II Plan (Blackham, 1989): 1) high-pressure, large-particle reactor design, fabrication and preliminary data; 2) experimental reaction rate data for chars from five coals. During the last quarter, personnel to work on this study were selected. The subtask is being closely coordinated with Subtasks 2.b and 3.b.

High-Pressure, Large-Particle Reactor Design

Introduction and Literature Survey - In the Phase II Plan for this subtask (Blackham, 1989), a test facility consisting of a TGA unit encased in a high-pressure shell was proposed. This suggestion followed the essential features of an experimental unit constructed by Sears et al. (1982). This facility is a pressurized thermobalance designed to operate at pressures up to 1000 psig at intermediate temperatures, or to almost 2000 K at one atmosphere.

The maximum conditions attainable simultaneously are reported to be 1570 K at 450 psig. Results are given for a lignite coal reacting with CO_2. The main objective for this equipment was to study coal pyrolysis and gasification reactions continuously at high temperature and pressure. A significant observation of their study was that "data of this nature are practically nonexistent for gasification reactions." In subsequent papers (Tamhankar et al., 1984; Sears et al., 1985) this facility has been used to study chars at up to 16 atmospheres at 1170 K reacting in CO_2 and H_2O. No data on reaction in oxygen were reported. Parikh and Mahalingan (1987) reported the use of a fixed-bed reactor to simulate conditions in the devolatilization zone of a Lurgi gasifier. The entering reactive gas contained 2 percent oxygen and 30 percent steam. The operating conditions were 600-800 K and 30 psig.

Kalson and Briggs (1985) studied the devolatilization of a single lump of coal (15 grams) at 100 kPa (14.7 psia) in the temperature range 700-850 K. The devolatilizer consisted of a 5.25 cm I.D. stainless steel pipe with the sample held in a 4.1 cm O.D. stainless steel screen basket. The basket was suspended on a chain that was raised or lowered within the devolatilizer pipe by means of an electrically controlled winch. It was indicated that the design of the unit could operate at a pressure of 1.7 MPa. It was also noted in their paper that "little systematic information is available for tar production from fixed-bed gasifiers."

Nuttall et al. (1979) reported on a bench-scale, single-particle reactor where internal conditions could be both controlled and monitored by a minicomputer. Coal samples (2.5 cm diameter) were used in devolatilization tests. "The coal particle was placed in a wire mesh basket attached to the force transducer by a stainless steel rod." Temperatures were measured by micro-thermocouples attached to the coal particle. Feldkirchner and Johnson (1968) described the construction of a high pressure thermobalance for study of iron ore in cycles of oxidation and reduction. They built this thermobalance to operate "at elevated pressures and temperatures because none were available commercially." The high pressure system consisted of two tubes joined together with the lower tube placed vertically in an electric furnace. The upper tube contained a microforce transducer of 10 g. capacity for weight measurement. A gold suspension chain is attached on one end to a windlass and on the other end to a nickel wire which supports the sample in a nickel mesh basket. The reactor tube was rated for heating to 1200 K. The complete system could be taken to a pressure of 100 atm.

The references briefly reported above are serving as the basis for our discussions concerning the experimental system to be designed and built for the fixed-bed oxidation studies of this subtask. Additional literature references have also been obtained and are being reviewed.

Selection of an Experimental Approach. On the basis of the experimental approaches reported in the literature, it was concluded that satisfactory reaction tubes can be designed and built which can be inserted into the HPCP reactor of Subtask 2.b. In this way, much of the facility needed for Subtask 2.f. already available. The general features of the large-particle design will consist of three components: a) the reactor tube, b) the balance, and c) the connecting pipe. The balance unit under pressure may include a magnetic bar suspending a platinum wire mesh basket by a long platinum wire. The suspending force can be controlled by a suitable external solenoid to give a record of mass loss of the sample in the basket. Alternatively, the entire balance unit may be encased to put all of the unit under pressure except the electronic control circuits passing through the pressure boundary. The connecting pipe will convey the pressure of the reactor to the balance unit and provide the housing for the long suspending wire. The connecting pipe may have a small pressure-sealed panel than can be easily opened to change samples. The suspending wire will be sufficiently long to place the sample in the optical access path at the lower part of the reactor. Different reactor tubes may be placed in the reactor to provide flexibility in the types of experiments envisioned. A ceramic tube may be necessary at the highest temperatures planned. Quartz tubes will be needed for the optical access for particle or bed temperature measurement. Pyrex tubes may be used at sufficiently low temperatures. A quartz tube with a bonded sintered disk may provide a platform for a bed of large particles.

Discussion and Evaluation of Design. The personnel of Subtasks 3.b. and 2.f. have met a few times during the quarter and discussed the features of the experimental approach outlined above. With a large char particle in a hot reactive gas stream, the surface temperature of the reacting particle may be considerably higher than the gas temperature. The optical system currently under construction for Subtask 2.b. will be used to determine the surface temperatures. Also, it may be necessary to place tiny thermocouples within the particle to follow the changes of temperature. The design of the balance unit will be given first priority. With samples in the 1-5 gram mass range it is desireable to follow changes in mass during reaction to the nearest

milligram. It will be necessary to determine if this can be achieved with hot gas flowing around the sample.

Different sample configurations are being considered: a) a single large particle - spherical, square, or cylindrical; b) a cluster of large particles held in a wire mesh basket; c) a long cylindrical particle with only the ends available to the reacting gas - hence one dimensional reaction; d) a bed of large particles on a sintered disk bonded to the reactor tube. Some checks on preliminary design features using some simple reactor tubes in a crucible furnace or a tube furnace at atmospheric pressure without optical temperature measurement are planned.

Experimental Reaction Rate Data

Experimental work has not yet been initiated.

Plans

During the next quarter, detailed design of the three components of the reactor tube insert will continue. Evaluation of some design features will be made using simple quartz tubes in a crucible or tube furnace at atmospheric pressure. Analytical methods and procedures will be determined for char characterization and for reaction rate calculations. Some large particle chars will be prepared under simple atmospheric pressure conditions.

II.G. SUBTASK 2.G. – SO_x/NO_x SUBMODEL DEVELOPMENT

Senior Investigators: L. Douglas Smoot and B. Scott Brewster
Brigham Young University
Provo, Utah 84602
(801) 378-4326 and (801) 378-6240

Research Assistant: Richard D. Boardman

Objectives

The objectives of this subtask are 1) to extend an existing pollutant submodel in PCGC-2 for predicting NO_x formation and destruction to include thermal NO, 2) to extend the submodel to include SO_x reactions and SO_x-sorbent reactions (effects of SO_3 non-equilibrium in the gas phase will be considered), and 3) to consider the effects of fuel-rich conditions and high-pressure on sulfur and nitrogen chemistry in pulverized-fuel systems.

Accomplishments

Much progress has been made toward verifying the expanded NO_x submodel. Work has primarily focused on evaluating the thermal NO mechanism incorporated into the code using the data collected under independent funding at BYU in a laboratory-scale reactor. Refinements to PCGC-2 have resulted in improved prediction of the temperature and major species concentrations. Subsequently, thermal NO predictions have been made and compared with the data. Additional experimental work has been carried out with independent funding to investigate the chemistry in the near-burner region of the reactor. Important findings have resulted from the joint theoretical and experimental work.

Options available for estimating radical oxygen have been partially investigated for the thermal NO model. Sensitivity of the rate expressions to temperature has been demonstrated. Improved coal gasification cases have been completed which closely match experimental data. An investigation of the expanded fuel NO mechanism is now ready to begin.

NO_x Submodel Development

Evaluation of Thermal NO Mechanism In the 7th Quarterly Report (Solomon et al., 1988b) the expanded NO_x submodel was presented along with data that were measured at BYU in natural gas and propane diffusion flames. Initial PCGC-2 simulations were presented which demonstrated deficiencies of the code in predicting the basic flame structure. This made it difficult to evaluate the thermal NO mechanism. After making corrections to the radiation submodel, predictions were made which favorably match the measured major species (CO_2, CO, and O_2), temperature, and velocity profiles. Subsequently, thermal NO predictions have been made and compared to the measured NO concentrations.

Refinements were also made to the experimental data (Boardman, 1990; Eatough, 1990) during the quarter. The reactor burner was redesigned to establish a symmetric flame in the combustor. Spatially resolved major species, temperature, velocity, and pollutants species profiles were then measured in the near-burner region where the reactions of interest appear to occur. Concentration of NO, NO_x, HCN and NH_3 was measured to determine if prompt NO formation occurs in the flame region.

Figures II.G-1 and II.G-2 compare predicted and measured major species and temperature for the natural gas/air combustion tests. The major species are shown to closely match the measured data in the near-burner region where temperature is maximum. In the aft region of the reactor, CO_2 is predicted above the measured concentrations while CO is predicted below the measured concentration. The sum of CO_2 and CO always equals the sum of the measured values. In all three radial profiles, predicted oxygen concentrations closely match the measured values. It is important to predict the correct magnitude and trend of the major species since radical oxygen concentrations are estimated from partial equilibrium assumptions involving the major species (Iverach et al., 1973; Sarofim and Pohl, 1973; and Thompson et al., 1981).

$$[O] = K'[O_2]^{1/2} \qquad \text{(II.G-1)}$$

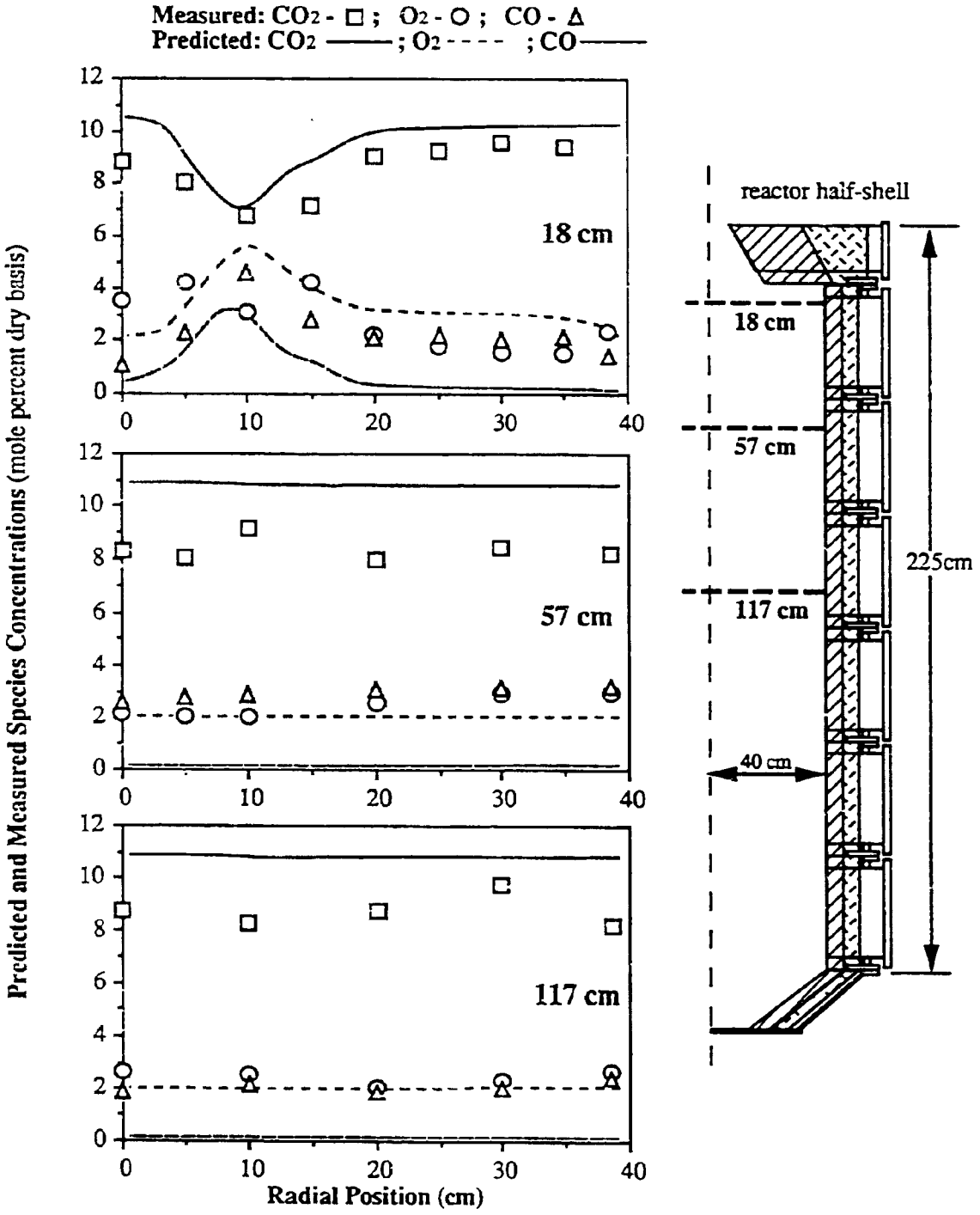

Figure II.G-1. Comparison of measured (symbols) and predicted (lines) major species radial profiles for a 500,000 BTU/hr natural gas/air diffusion flame.
Equivalence ratio = 0.98; Secondary swirl number (theoretical and actual) = 1.5;
Data measured in a BYU Advanced Combustion Engineering Research Center reactor (Eatough, 1989).

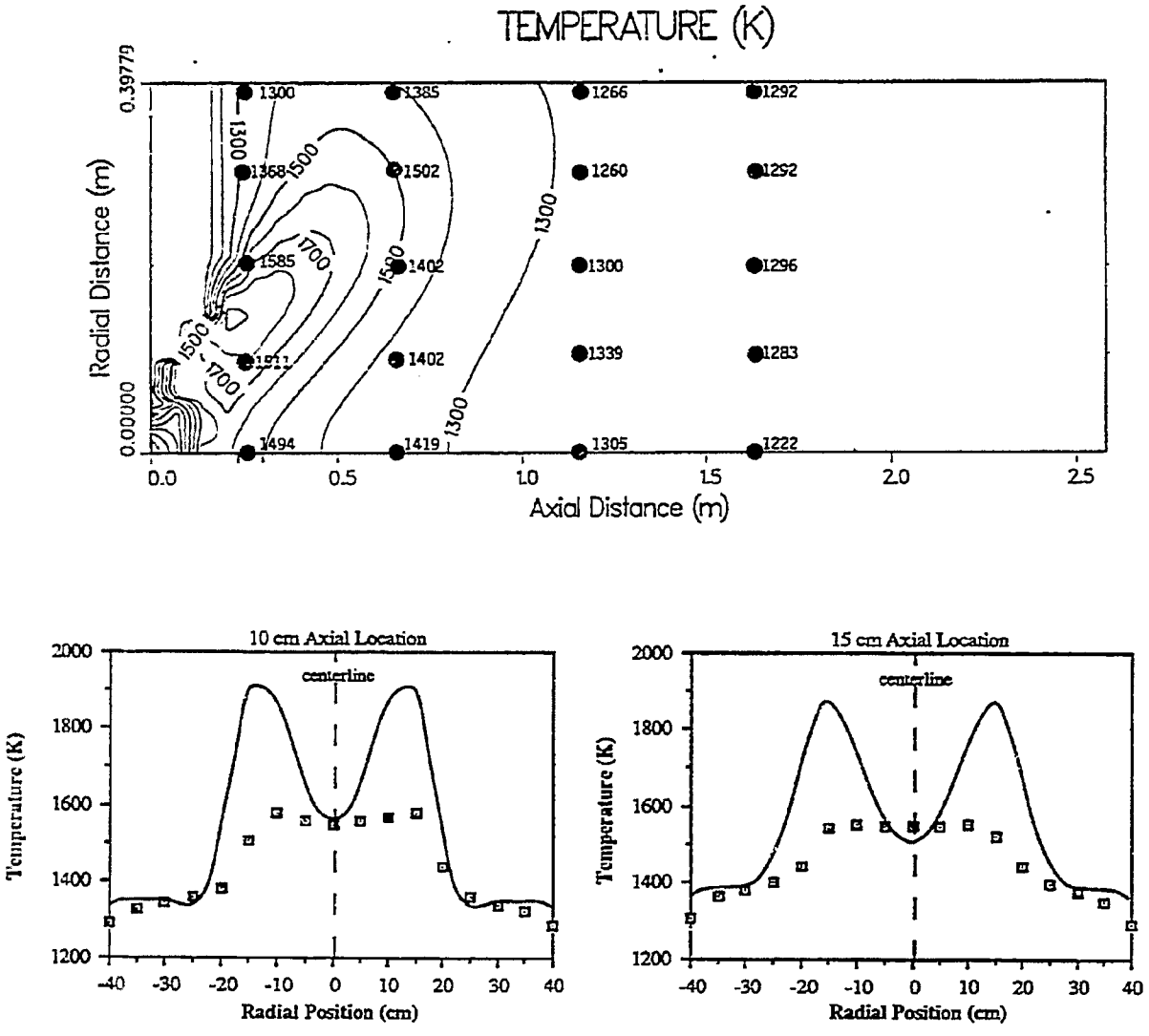

Figure II.G-2. Comparison of measured (symbols) and predicted (curves) temperature profiles for a 500,000 BTU/hr natural gas/air diffusion flame. Equivalence ratio = 0.98; Secondary swirl number = 1.5; Data measured in a BYU Advanced Combustion Engineering Research Center reactor (Eatough, 1990).

$$[O] = K^{*}[O_2][CO]/[CO_2] \qquad \text{(II.G-2)}$$

Figure II.G-2 reveals that the predicted temperature field generally matches the experimental data except in the peak temperature region. A shielded suction pyrometer was used to obtain the measured values, and there is a possibility that the intrusive nature of the probe disturbed the fluid mechanics significantly. This would presumably lead to decreased mixing and decreased reaction in the highly turbulent near-burner region resulting in a low temperature measurement. Furthermore, the measured data are uncorrected for heat loss of the thermocouple pile to the pyrometer shield and probe. According to calculations, a heat balance would adjust the measured temperature upward by as much as 50 K. Despite the early disparities between the predicted and measured temperature profiles, agreement of the temperature along the reactor wall and centerline and at the combustor exit infers the reactor heat balance closes. Any adjustment to the wall boundary temperatures resulted in predicted temperatures fields which did not match the composite temperature field as well. Thus, the predicted temperature field was thought to be suitable for evaluating the NO_x submodel.

Figure II.G.3 presents detailed measurement of nitrogen pollutant species and compares the predicted and measured NO concentrations throughout the reactor. Predicted NO concentrations were made using the extended Zeldovich mechanism. Radical oxygen concentrations were estimated assuming oxygen radicals to be in partial equilibrium with O_2 (Equation II.G-1). When radical oxygen concentrations were estimated using Equation II.G-2, the predicted NO level was an order of magnitude higher (see Figure II.G-5, below). Even when the temperature was artificially adjusted down by 100 K, Equation II.G-2 led to NO predictions well above the measured profiles. It appears that it is most appropriate to use Equation II.G-1 to estimate oxygen radical concentration.

Figure II.G-3 shows the buildup and decay of HCN and NH_3 by interaction of fuel fragments (CH_i's) with molecular nitrogen and intermediate nitrogen species. The goal of the experimental work was to operate at conditions where prompt NO and NO_2 formation would be minimized. This attempt was thwarted due

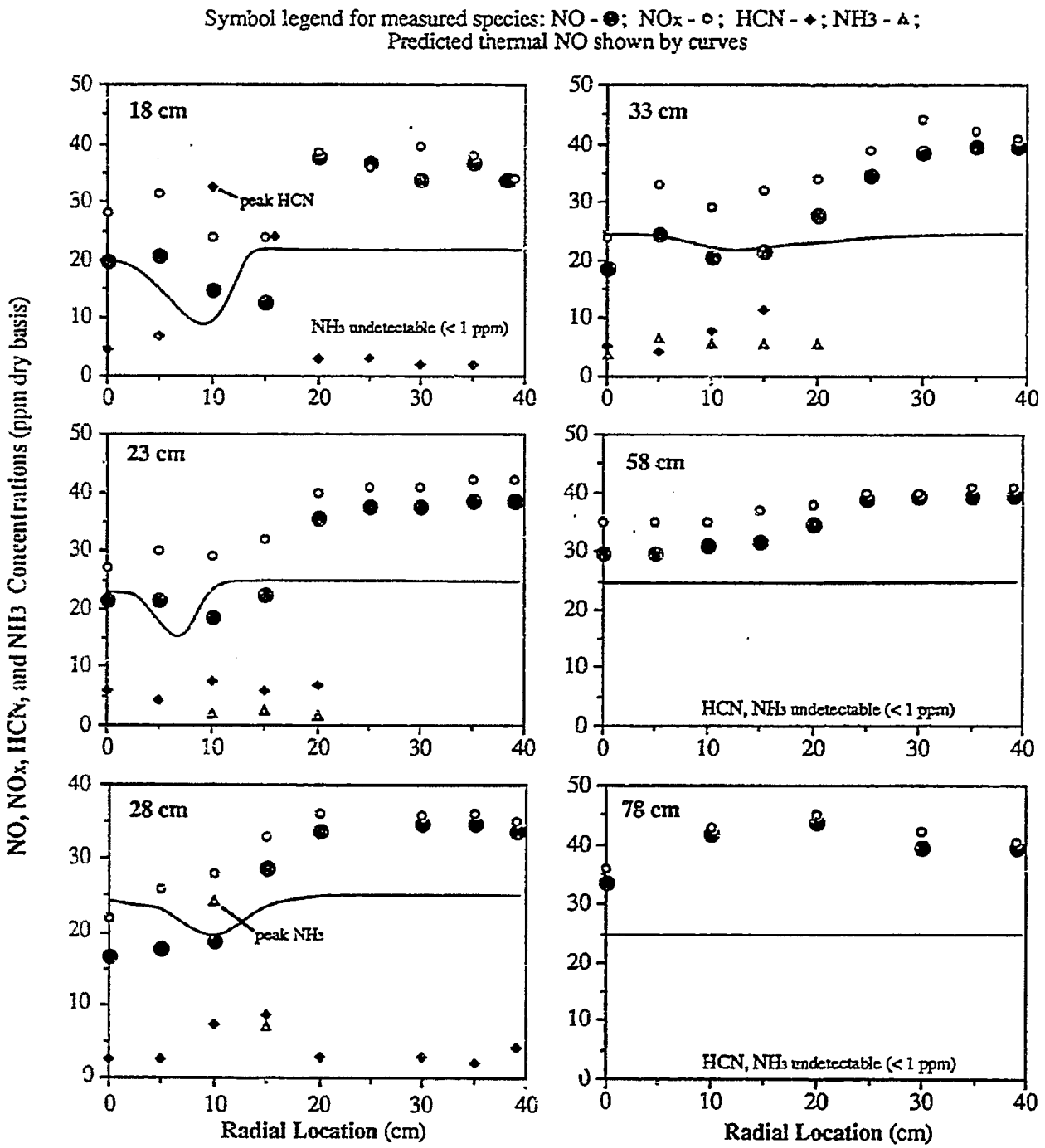

Figure II.G-3. Comparison of predicted thermal NO (——) with measured NO (●) for a 500,000 BTU/hr natural gas/air diffusion flame. Axial location of radial profiles listed in upper left corner. Other measured species (NO_x, HCN, and NH_3) shown to demonstrate complexity of the chemistry. Data measured in a BYU Advanced Combustion Engineering Research Center reactor. Equivalence ratio = 0.98; Secondary air swirl = 1.5

to the locally fuel-rich zone inherent in non-premixed flames. Thus, it is impossible to completely avoid mechanisms of prompt NO formation and decay in hydrocarbon diffusion flames.

Figure II.G-4 illustrates the complex mixing structure established when swirl is imparted to the secondary air stream. A fuel-rich region exists along the flame front where HCN is produced. Figure II.G-3 shows that HCN passes through a maximum at the flame edge. The highest observed HCN concentration occurred on the 18 cm radial profile. Higher values may occur in the reactor quarl. NH_3 builds up as a result of HCN decay. This trend is observed in the experimental data which show initially undetectable quantities of NH_3 and then buildup at later profiles. The highest NH_3 concentration is not observed until 28 cm. These measurements are consistent with measurements of Mitchell et al. (1980) in a laminar methane/air diffusion flame, although a higher level of NH_3 was detected in the experiments of this work.

The detection of relatively large concentrations of cyanide and amine components reveals that NO is formed from HCN and NH_3 oxidation on the fuel-lean side of the flame front. This mechanism of NO formation is termed "prompt NO" since it occurs early in the reactor where radical fuel species are present. NO is also reduced to N_2 by nitrogen intermediates on the fuel-rich side of the flame. Figure II.G-4 depicts the global reactions for the reactions occurring along the flame front. There is a possibility that the formation of NO by the prompt NO reactions is compensated or exceeded by the destruction of NO by nitrogen intermediates in the fuel-rich core.

The nitrogen chemistry is further complicated by the formation of NO_2, which is the majority of the difference between NO_x and NO concentrations shown in Figure II.G-3. NO_2 is formed by oxidation of NO by HO_2 in fuel-rich regions. It is subsequently converted back to NO by reaction with H radicals. The measured data show that NO_2 is formed in the fuel-rich recirculating zone and then is essentially all converted back to NO shortly following uniform mixing in the reactor.

The purpose of these comparisons is to demonstrate the ability of the Zeldovich mechanism to predict thermal NO formation. The predicted thermal NO

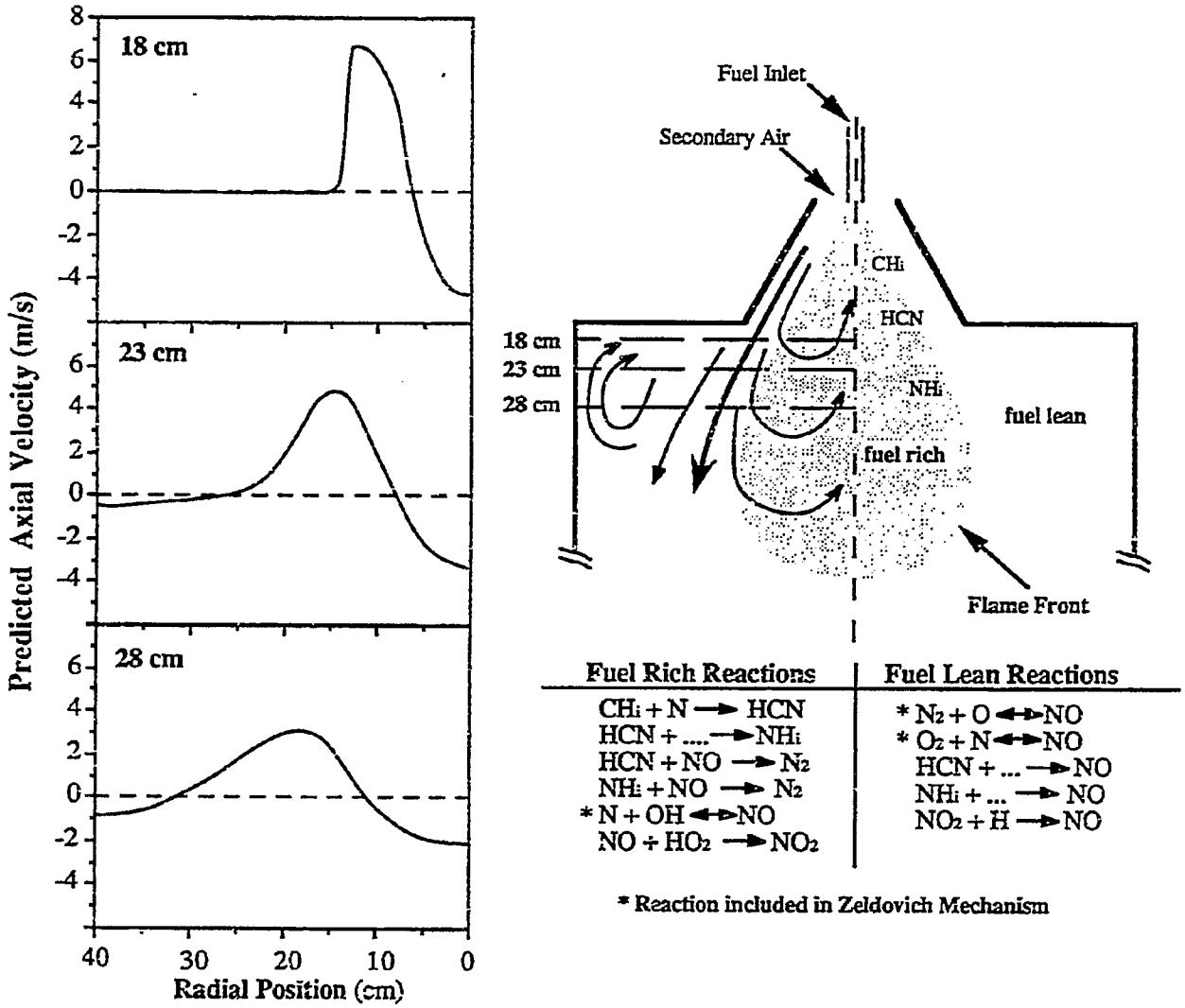

Figure II.G-4. Schematic showing mixing and nitrogen chemistry in the near burner region of a swirling-flow, natural gas/air diffusion flame. Velocity profiles predicted by PCGC-2 show recirculation strength near the wall and at the center region of the reactor.

is lower than the measured concentrations by approximately 30 percent. Whether this difference is due to prompt NO formation remains uncertain. In general, a limitation of using the NO_x model to predict NO formation in gas combustors has been identified. Aside from these complexities, the thermal NO appears to predict NO concentrations on the order of the measured values.

The sensitivity of the thermal NO mechanism to temperature is demonstrated in Figure II.G-5. Predictions were made using the base solution with uniform adjustment to the temperature field. The single point at [0.0, 485] was made using Equation II.G-2 to estimate radical oxygen concentrations. This demonstrates one application of the code to predict the effect of increasing the reactor temperature.

The greatest utility of the code will be realized if the thermal NO mechanism can match observed trends that were measured during parametric variation of equivalence ratio and secondary swirl number. These predictions are currently being made and will be reported in the next quarterly report. Additional work is in progress to predict data measured in a separate natural gas-fired combustor that were obtained from TECFLAM in West Germany.

Fuel NO Mechanism Evaluation - Subsequent to revisions in the radiation submodel of PCGC-2, a lignite coal gasification case has been predicted. Work is ready to begin during the next quarter to evaluate the available options of the expanded fuel NO mechanism. Additional cases for coal combustion will be evaluated using the improved code.

SO_x-Sorbent Reactions Submodel Development

Simulations of gasification cases are in progress to determine the validity of using an equilibrium approach when predicting SO_x species under fuel-rich conditions. These results will be presented and discussed in the next quarterly report.

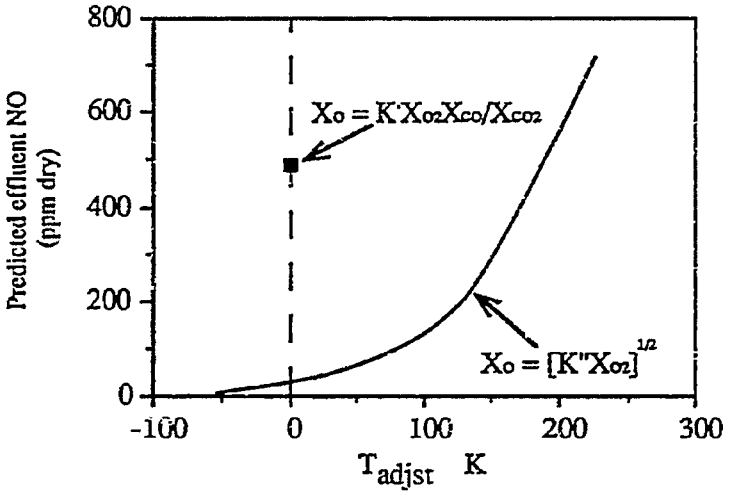

Figure II.G-5. Predicted thermal NO concentrations using the extended Zeldovich mechanism. T_{adjst} represents a uniform temperature adjustment to the predicted field of temperatures shown in Figure II.G-2 (T_{adjst} = 0.0 matches the predicted temperature field). Symbol at [0.0, 485] was predicted using Equation II.G-2.

Plans

Work during the next quarter will continue to focus on evaluation of the NO_x submodel. The evaluation of the revised and expanded NO_x submodel will be completed and reported in the next quarterly report. Emphasis will be given to predicting NO trends with increasing stoichiometric ratio and swirl number variation. Comparisons will also be completed for the data procured from TECFLAM (KäB, 1989). Concurrently, low rank coal combustion and gasification simulations will be made to further investigate the empirical fuel and thermal NO mechanism adapted from Mitchell and Tarbell (1982). The expanded version of the original fuel NO mechanism of Smith et al., (1982), which now includes NH_3 as a reaction center, will also be tested. A comparison of predicted and measured SO_2 and H_2S species will be made for the coal gasification simulations completed during the NO_x model evaluation. Modifications to PCGC-2 to generalize the feed inlets will then begin.